Microstructural Effects Regarding Fracture of Clinically Retrieved Dental Sonic and Hand Scalers

H. J. Mueller
American Dental Association

M. S. Bapna
University of Illinois

Recommended Citation

Mueller, H. J. and Bapna, M. S. (1997) "Microstructural Effects Regarding Fracture of Clinically Retrieved Dental Sonic and Hand Scalers," *Cells and Materials*: Vol. 7 : No. 2 , Article 1.
Available at: https://digitalcommons.usu.edu/cellsandmaterials/vol7/iss2/1

Utah State University
MERRILL-CAZIER LIBRARY

MICROSTRUCTURAL EFFECTS REGARDING FRACTURE OF CLINICALLY RETRIEVED DENTAL SONIC AND HAND SCALERS

H.J. Mueller[1] and M.S. Bapna[2]

[1]Department of Dental Biomaterials, American Dental Association, 211 East Chicago Avenue, Chicago, IL
[2]Div. Biomaterials, Dept. Restorative Dentistry, School of Dentistry, University of Illinois at Chicago

Abstract

The fracture surfaces of sonic and hand scaler instruments fractured under clinical and laboratory conditions were compared to their etched sections, and analyzed for evidence revealing the process that led to their failure. Scanning electron microscopy and energy-dispersive spectroscopy indicated the quality of the martensitic stainless steel comprising the sonic scalers, all from one manufacturer, was inferior to the steel comprising the hand scalers from another manufacturer. The sonic scalers contained stringer inclusions aligned longitudinally and consisting of calcium, aluminum, silicon, and other elements up to 50 μm in length. The sonic scalers displayed brittle fracture while the hand scalers displayed mainly ductile fracture. Microcracks occurred between stringer inclusions. Microhardness for sonic scalers, although slightly higher and significantly different from hand scalers, proved ineffective for detecting a structure-property relationship. Microscopy, however, proved very useful for this purpose and also well-suited for analyzing the stress state occurring on the instruments at the time of failure. All sonic scalers were stressed by being bent inwards, while a hand scaler was pulled and torqued by twisting. Retained coarse grinding grooves also affected fracture. Recommendations are made for hand instrument standards to include checks on steel quality for inclusions of the stringer type.

Key Words: Dental sonic scalers, hand scalers, martensitic stainless steel, carbide, fracture, brittle, ductile, hardness, toughness, bending, torsion.

*Address for correspondence:
Herbert J. Mueller
American Dental Association Health Foundation,
Paffenbarger Research Center, Building 224,
National Institute Standards and Technology,
Gaithersburg, MD 20899
Telephone no.: (301) 975-4344 / FAX: (301) 963-9143
E-mail: herb.mueller@nist.gov

Introduction

Breakage of dental hand instruments during patient therapy has the potential to harm the patient and result in litigation against the practitioner and instrument manufacturer. Although instrument parts that fracture in patients' mouths are most often retrieved, there have been several reports indicating the serious inconveniences to the patients that can arise: endoscopic removal of a dental instrument part from the colon (Thomas and Carr-Locke, 1989) and foreign bodies of dental origin in the alimentary and respiratory tracts (Littner and Dayan, 1982), esophagus (Nandi and Ong, 1978; Szabo et al., 1972), and gastrointestinal tract (Ioannidis, 1990). The patients' health and well-being can be in serious jeopardy if such foreign bodies are not removed.

Breakage of a tip from a hand instrument, such as a scaler or curette, resulting in a loose instrument part in the patients' mouth, must be regarded as an emergency situation. At least momentarily, this is a more serious situation than a fractured endodontic instrument remaining fixed within a root canal of a tooth. By caution, and common sense measures, the practitioner can quickly remedy the situation (Carroll, 1993).

In order to obtain hardness, toughness and other mechanical properties necessary for these instruments to maintain sharpened edges, desired angles and pointed tips and, at the same time, resist fracture and wear, carbon steels and stainless steels are used in scaler fabrication. Composition and metallurgical processing of these steels control their final properties. The importance of metallurgical processing must be highlighted, since various thermal procedures such as annealing, quenching, and tempering heat treatments are used that must be closely controlled for steels of particular compositions. Differences in hardness profiles between carbon and martensitic stainless steel dental hand instruments were reported (Gettlemen and Renz, 1981), and hardness was found to vary among similar instruments from different manufacturers (Geaman and Moser, 1987). While these reported property differences may still correspond to steels with properties for optimum dental performance,

the dental literature provides no information about effects from metallurgical processing variables on dental instrument performance. National {ANSI/ADA No. 29 (1976) and No. 64 (1986)} and international {ISO 7153/1 (1983) and 683/13 (1986)} specifications on instruments provide for a wide range in instrument properties. Accordingly, manufacturers must rely on independent analyses and their own unpublished data if they wish to produce hand instruments with optimum properties for dental use.

Breakage of dental scalers occurs by the application of force, either by pulling, pushing, twisting, bending or a combination of modes. Increasing instrument hardness and brittleness by controlled metallurgical processing produces instruments with higher yield and breakage strengths and toughnesses. However, uncontrolled instrument processing can lead to scalers that are too brittle, fracture at low levels of strain and absorb very little energy prior to fracture. Instruments for optimum dental usage have high hardness and brittleness, yet also absorb a high level of energy. This combination of properties results in instruments that maintain sharpened edges over extended times. Although not reported in the literature, instrument breakage at lower than normally anticipated loads due to inferior quality has been experienced by many clinicians. While most manufacturers have selected mechanical properties providing for optimum clinical performance, variations in the supply of steel and in its processing are not uncommon and can lead to inferior products if not detected by stringent control measures. The dental literature has not dealt with force levels required to break dental instruments. ANSI/ADA Specification No. 64 deals somewhat with this issue by specifying hardness limits for martensitic stainless steels used for the working end of dental instruments. The specification is based on ISO terminology (ISO 7153/1) for steels used with different surgical instruments.

The goal of this project was to analyze the fracture surfaces of clinically retrieved sonic and hand scalers for the purpose of obtaining information regarding the reason for *in vivo* failure of these instruments.

Materials and Methods

Clinically retrieved hand instruments were obtained from two sources. The first source was a dentist who provided three broken sonic scalers (Titan-S incorporating a universal tip; Star Dental Manufacturing Co., Valley Forge, PA) with the mating broken tips and an intact unused tip, all from the same lot. The submitted broken instruments had failed during clinical usage very shortly after commencing scaling. The practitioner insisted that failure occurred after barely touching the instrument tips to teeth. Other facts included an air pressure line connected to the scaler unit of 0.25 MPa, which was within specification, and steam autoclaving of the instrument tips according to standardized procedures. The second source was several clinical faculty members from a dental school who had experienced instrument breakage. From this source, two clinically broken hand scalers, types No. S204S and No. SH6/7 (Hu-Friedy, Chicago, IL), were selected from a larger collection of broken instruments for further laboratory analysis. In addition, new scalers of types S204S and SH6/7 (Hu-Friedy) were purchased from a dental supplier.

Vickers microhardness of selected instruments was determined. Two Titan-S sonic scalers, one clinically fractured and the other in the unused condition, and one each of the S204S and SH6/7 hand scalers in the clinically fractured condition were tested. The broken instrument tips were first mounted lengthwise in epoxide resin, followed by routine metallographic grinding and polishing procedures. After grinding with 120 grit silicon carbide abrasive paper until approximately one-half of the instrument diameter remained, further grinding was performed with 240, 320, 400, and 600 grit papers. Polishing followed using alumina slurries with 12.5, 5.0, 1.0, and 0.3 μm particles. The mounted and polished instrument tips were then evaluated using a Tukon microhardness tester (Acco Wilson Instrument, Bridgeport, CT) with an applied load of 500 g. The microhardness tester was calibrated with a standardized hardness block (Acco) having a Vickers hardness of 742. All microhardness readings reported are the mean of 10 individual readings randomly taken along the entire length of the mounted instrument. For selected instruments, mean values were obtained at specific locations over the cross-sections of the instruments, that is, within the interior, near the surface, near the instrument tip, and near the plane where the instrument fractured. Statistical comparisons were first performed with analysis of variance (ANOVA) by using the software program Statistix (Analytical Software, St Paul, MN), followed by pairwise comparison of means using the Tukey HSD test with an α level of 0.05.

Microstructural analysis of both the fracture surfaces and polished cross-sections used for microhardness measurements was performed by scanning electron microscopy (SEM) and digital energy-dispersive spectroscopy (EDS) with a conventional X-ray detector (Mueller, 1996). Except where noted, secondary electron images were monitored. The fracture surfaces of the hand instruments were first ultrasonically cleaned in acetonitrile to eliminate debris and loose particles, while the polished cross-sections were chemically etched with freshly made Vilella's reagent (Vander Voort and James, 1985), which contained 0.09 mM picric acid, 1 mM HCl

Figure 1. Broken scalers: (a) sonic, (b) SH6/7 hand, (c) S204S hand.
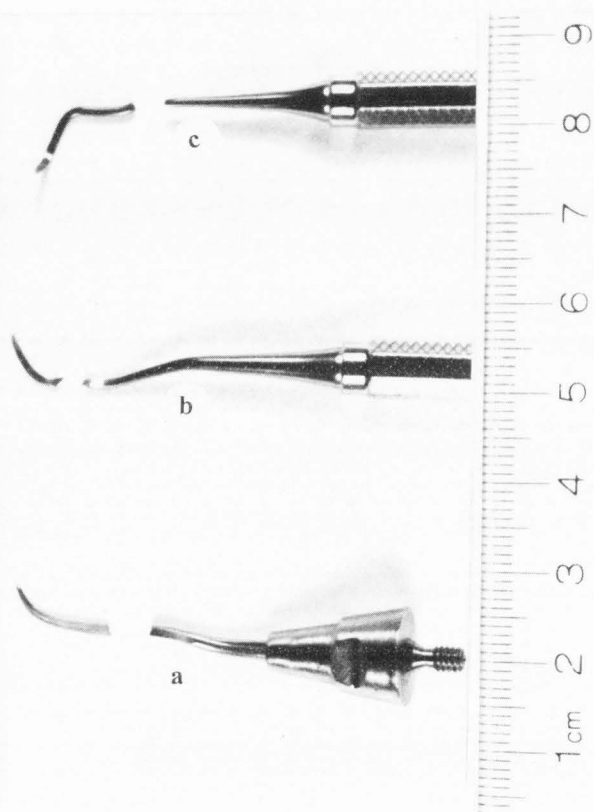
----

and 20 mM ethanol, by immersion at room temperature for up to one minute. For fractographic analysis, the fractured instruments and broken-off tips were mounted within the SEM chamber with the use of a stainless steel set-screw and aluminum holding device, while electrical contact between the resin-mounted samples and the aluminum mounting stubs was achieved with silver paint. Prior to insertion into the SEM chamber, all surfaces were submitted to a pressurized argon (grade 5.2) blast. All EDS spectra were collected for a total of 200,000 counts. Semi-quantitative compositional analysis was performed with a software program utilizing atomic number, absorbance, and fluorescence (ZAF) corrections. The pertinent instrument parameters included take-off angle of 10°, working distance of 25 mm, and accelerating voltage of 20 kV.

Results

Figure 1 shows broken scaler instruments, including both the main scaler piece and the smaller tip piece. For all of the sonic scalers (Fig. 1a), clinical fracture occurred about 10 mm from their tips. Fractures occurred within the instrument length where the cross-section was still square in configuration. At about 15 mm
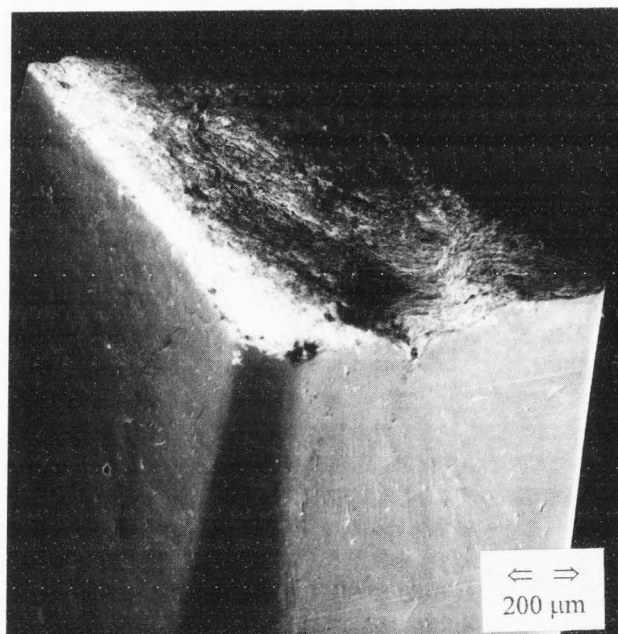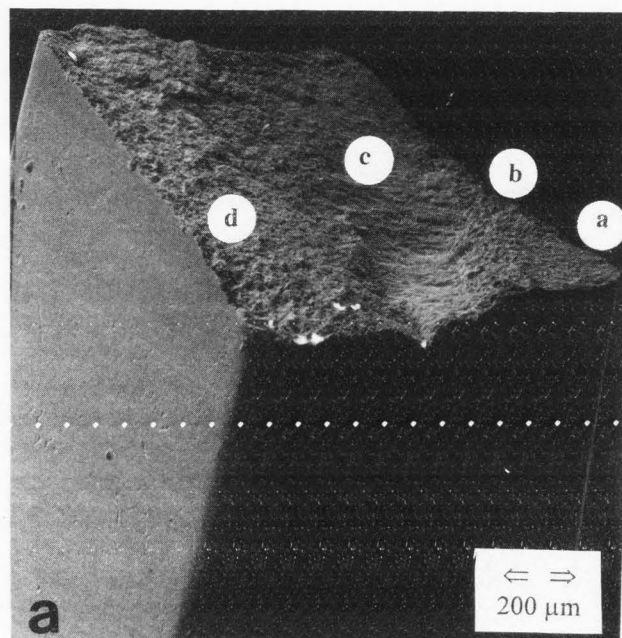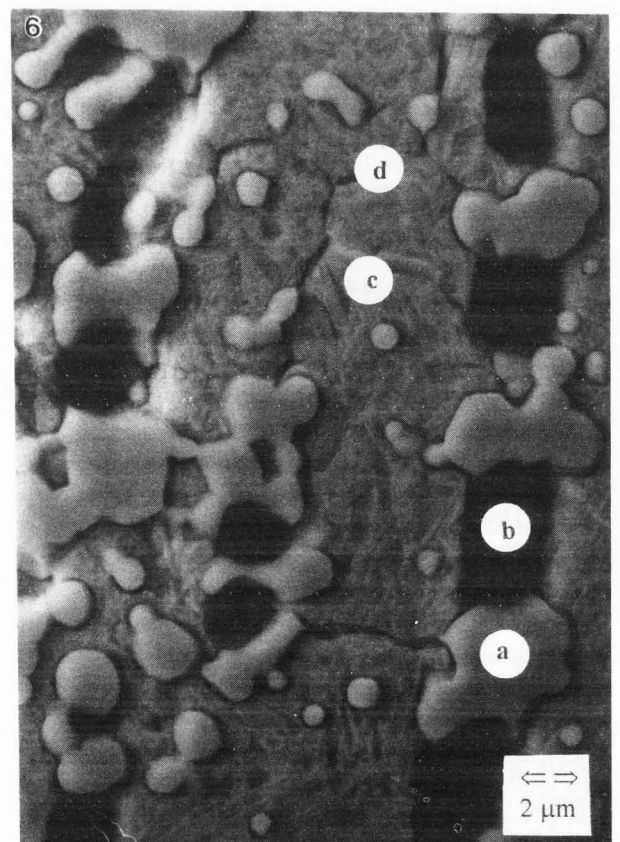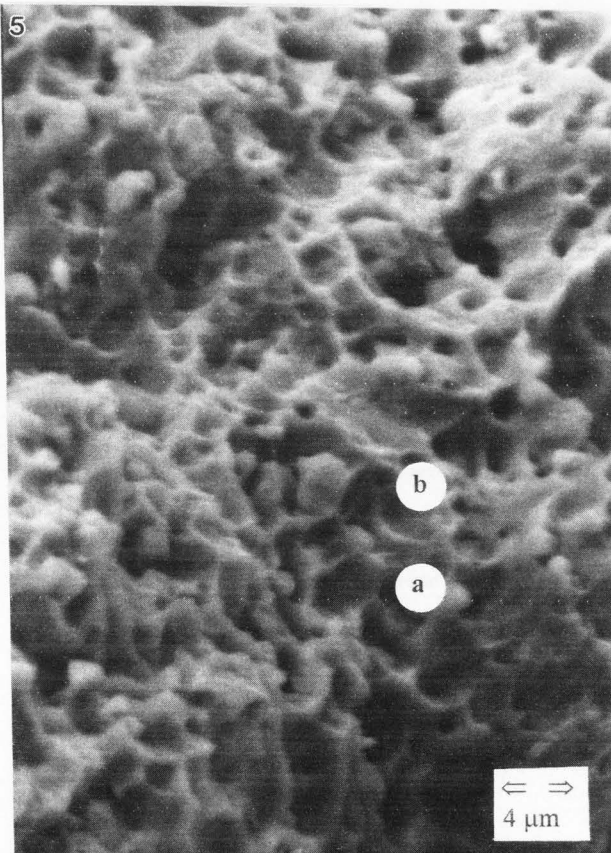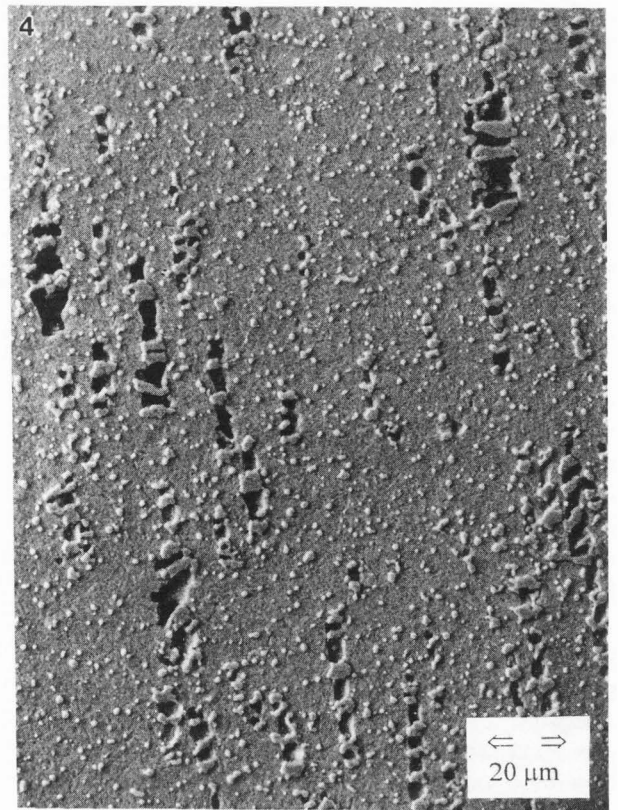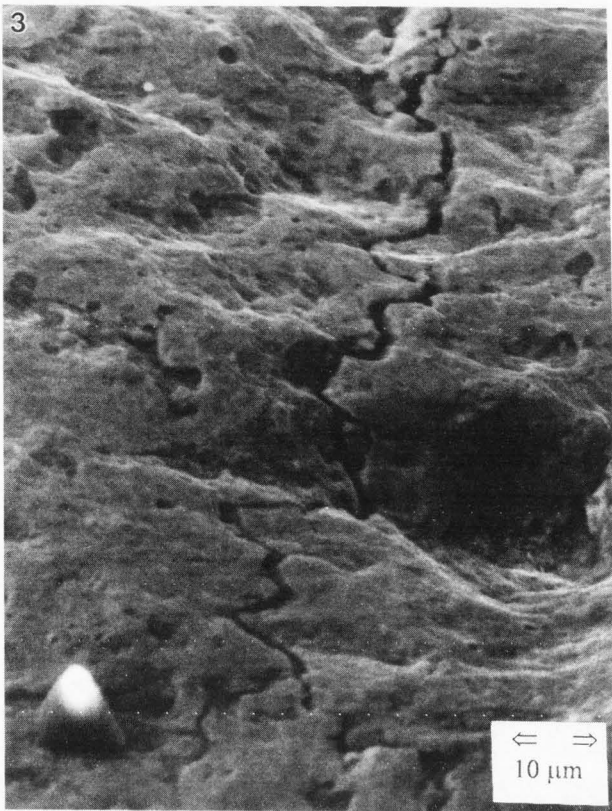

Figure 2. Scanning electron micrographs. (a) Secondary electron image of the fracture surface from a clinically retrieved broken sonic scaler showing regions (a), (b), (c), and (d). (b) Negative voltage bias image, the instrument sides are shown with better clarity than in Figure 2a.

----

from the instrument tip, the square cross-section changed to circular. For the SH6/7 scaler (Fig. 1b), fracture also occurred about 10 mm from its tip, just before the cross-section changed from the four-sided geometry to circular. For the S204S scaler, clinical fracture likewise

Figures 3 to 6 on the facing page

Figure 3. Higher magnification scanning electron micrograph of region c from the fracture surface shown in Figure 2a.

Figure 4. Higher magnification scanning electron micrograph of region d from the fracture surface shown in Figure 2a. Particle: a; dimple: b.

Figure 5. Scanning electron micrograph of polished and etched section of sonic scaler. Longitudinal axis of instrument runs lengthwise. Carbide particles and stringer inclusions (phase removed by etching) in matrix of martensite. Phases are identified in Figure 6.

Figure 6. Higher magnification scanning electron micrograph of Figure 5. Carbide particles: a; etched-out stringer inclusions: b; platelets of martensite within grain interiors: c; grain boundaries: d.

---

occurred about 10 mm from the tip, just before the second bend where a circular cross-section occurred. This scaler type has ground flat sides extending from the tip to just past the first bend. The fracture shown in Figure 1c for an S204S instrument, located about 20 mm from the tip well past the second bend, occurred in a laboratory bend specimen.

Figures 2a (secondary electron) and 2b (negative voltage bias) present low magnification micrographs of the fracture surface from a clinically retrieved sonic scaler. Figure 2b depicts, with better clarity, the condition of the instrument sides and reveals numerous microcracks running mostly in a longitudinal direction. The fracture surface is distinguished by four regions: (1) region a, the first stage of fracture, represents crack initiation from the bottom corner, positioned on the convex side of the instrument curvature, and extending a short distance inwards; (2) region b corresponds to a halo region extending a short distance beyond region a; region b has a more granular appearance and is partially slanted; (3) region c covers the largest area percent of the fracture surface and contains features running in the direction of fracture; the microscopic flatness of region c is depicted in Figure 3, the crack running lengthwise through the center of the micrograph extends, with reference to Figure 2a or 2b, radially from the deepest depression on the left to almost the mid-length of the right-bottom side; and (4) region d, shown in Figure 4, covers the topmost part of the fracture surface and is characterized by a granular appearance with particles often at the center of dimples.

Figures 5 and 6 present scanning electron micrographs of a polished and etched longitudinal section from the fractured sonic scaler tip shown in Figures 2, 3 and 4. Microstructural characterization of the remaining two
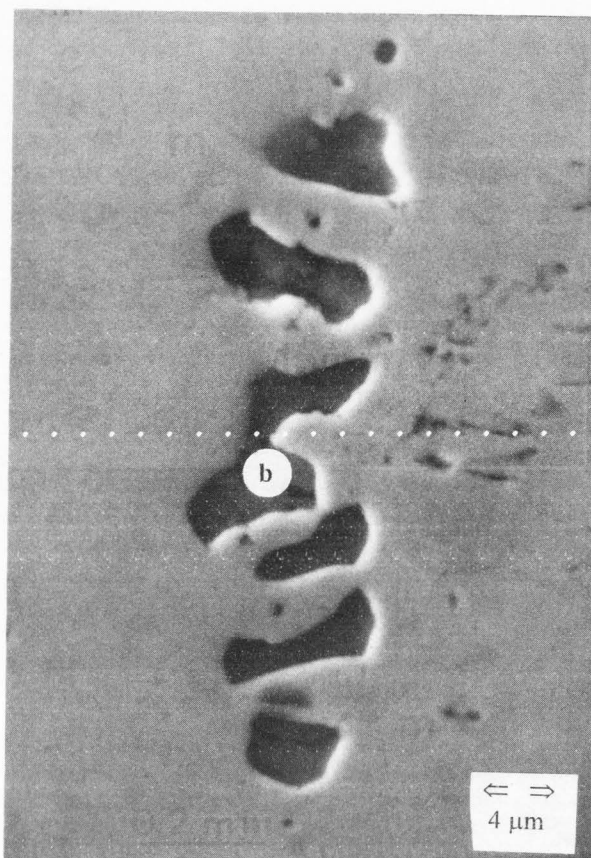

Figure 7. Scanning electron micrograph of polished only section of sonic scaler. Longitudinal axis of instrument runs lengthwise. The darker irregular areas (b) within center of micrograph correspond to material within stringer inclusion. These correspond to the areas that were etched out and shown as dark patches or voids in Figures 4 and 5.

---

fractured sonic tips and the new unused sonic tip revealed similar microstructures. All of the sonic tip microstructures contained particles of both smaller and larger sizes, grains, platelets within grains, and porosity shown as dark patches separated by particles and arranged lengthwise along the longitudinal instrument axis. A polished unetched section, shown in Figure 7, clearly revealed that the etched-out patches in Figures 5 and 6 consisted of inclusions. Particles of larger sizes were associated with the inclusions, in contrast to smaller particles located along grain boundaries and still smaller particles located within grain interiors.

EDS spot analyses (Fig. 8) of the microstructural constituents, shown in Figures 5 and 6, revealed the particles to be rich in Cr, with lower Fe, and with a small but detectable amount of S, while the matrix was rich in Fe but with lower Cr. Semi-quantitative analysis with a software program utilizing ZAF corrections revealed
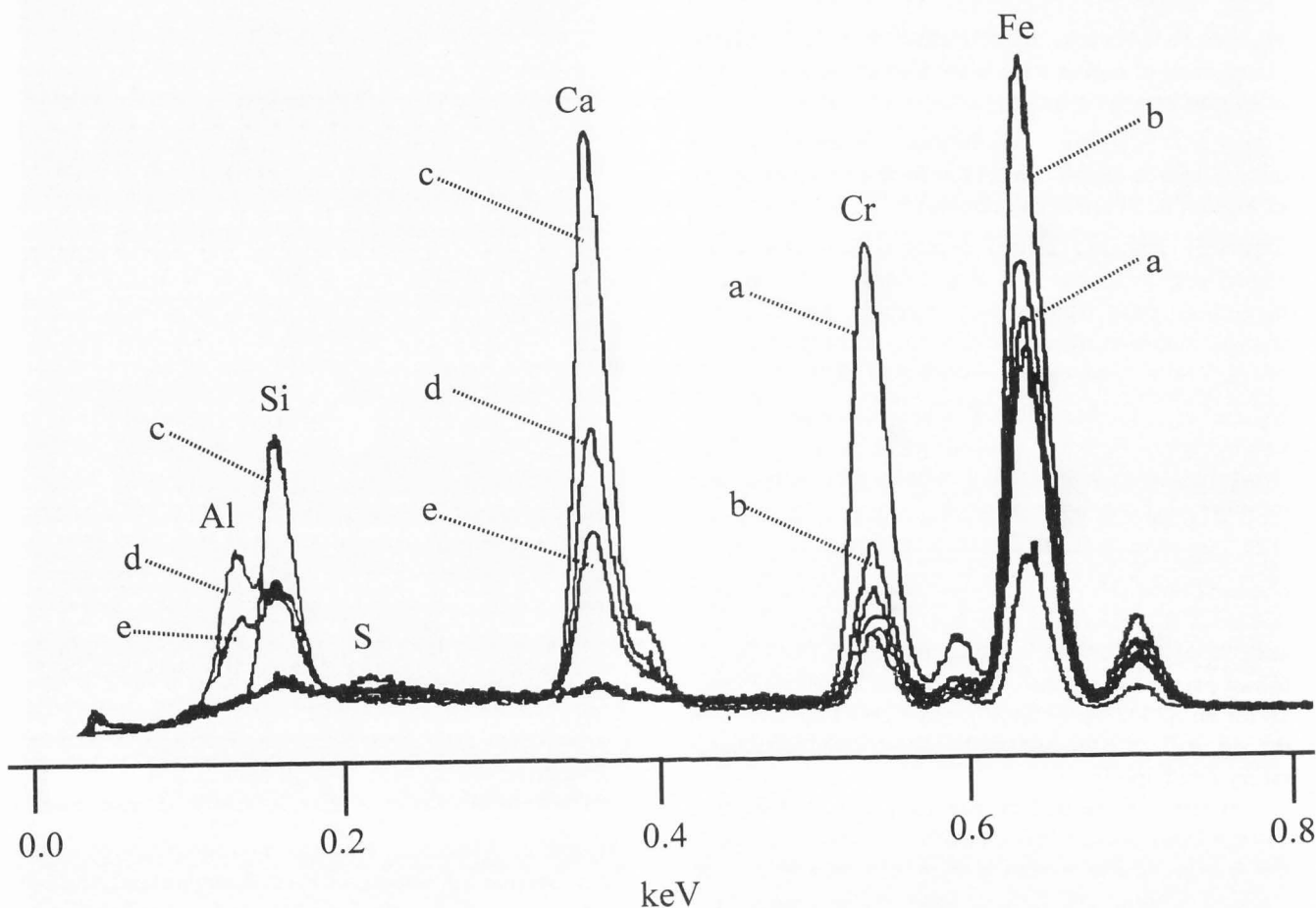
Figure 8. EDS spectra of carbide (a) and matrix (b) phases of polished and etched section from sonic scaler (Figure 5) and three spectra (c, d, e) from different spots of stringer material (Fig. 6). Full scale equals 3900 counts.

the composition of the particles by mass fraction to be 55-60% Cr, 40-45% Fe, and 0.5-1.0% S, and the matrix to be 15.5-16.0% Cr with the balance Fe. No distinctions were found in composition between the larger and smaller particles. EDS spot analyses of the inclusions shown in Figure 7 are also presented in Figure 8. Since variations in spectra occurred depending upon spot location in the stringer, a number of representative spectra are presented. Besides detection of Cr and Fe, the inclusions also contained Ca (at times, high levels) and low to moderate levels of Si and/or Al.

EDS spot analyses for constituents on the fracture surfaces for sonic and hand scalers yielded spectra similar to those for the particles and matrix from the polished and etched surfaces. The particles and surrounding dimples shown in Figure 4 correspond, respectively, to particles and matrix from the etched surface. Analysis of the microscopic flat regions, shown in Figure 3, yielded spectra similar to those for the particles and matrix. Spot analyses of selected particles and regions

Figures 9-12 on the facing page

Figure 9. Scanning electron micrograph of fracture surface from clinically retrieved S204S hand scaler showing regions (a), (b), (c), and (d).

Figure 10. Higher magnification scanning electron micrograph between regions b and c from the fracture surface shown in Figure 9.

Figure 11. Higher magnification scanning electron micrograph of region c from the fracture surface shown in Figure 9. Primary carbide (a), secondary carbide with small dimple (b), and left side of dimple surface emanating from primary carbide (c).

Figure 12. Higher magnification scanning electron micrograph of region d from the fracture surface shown in Figure 9.
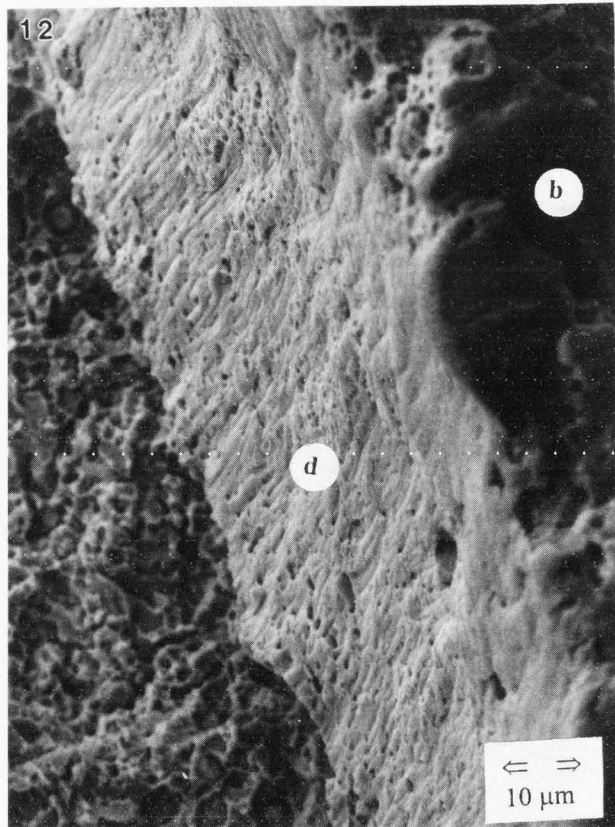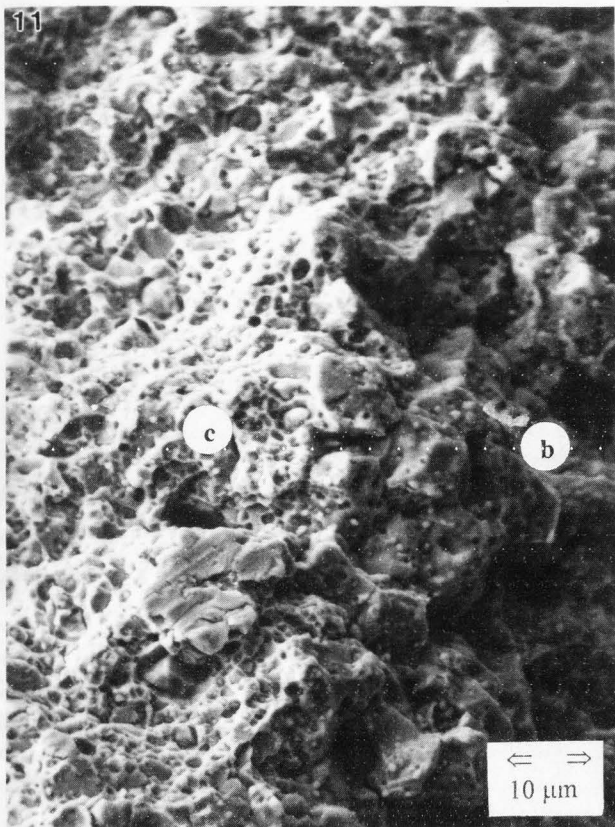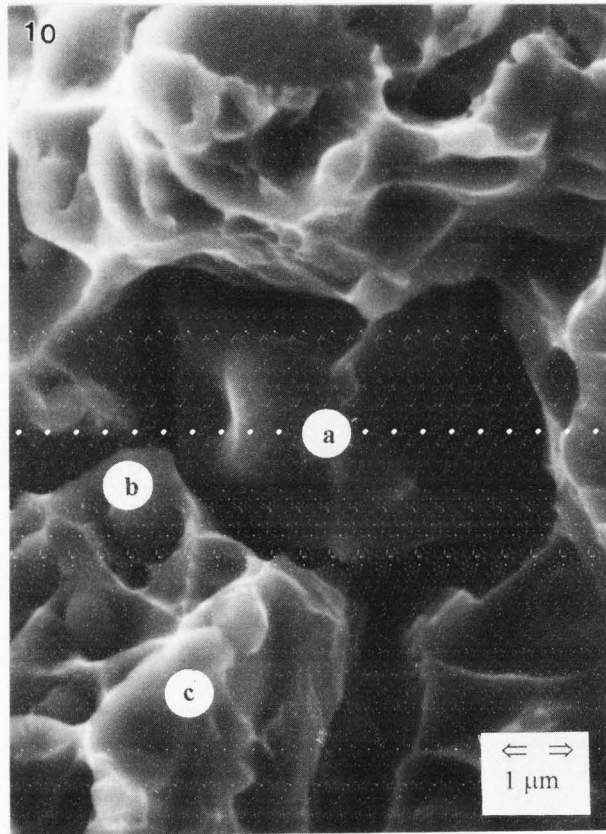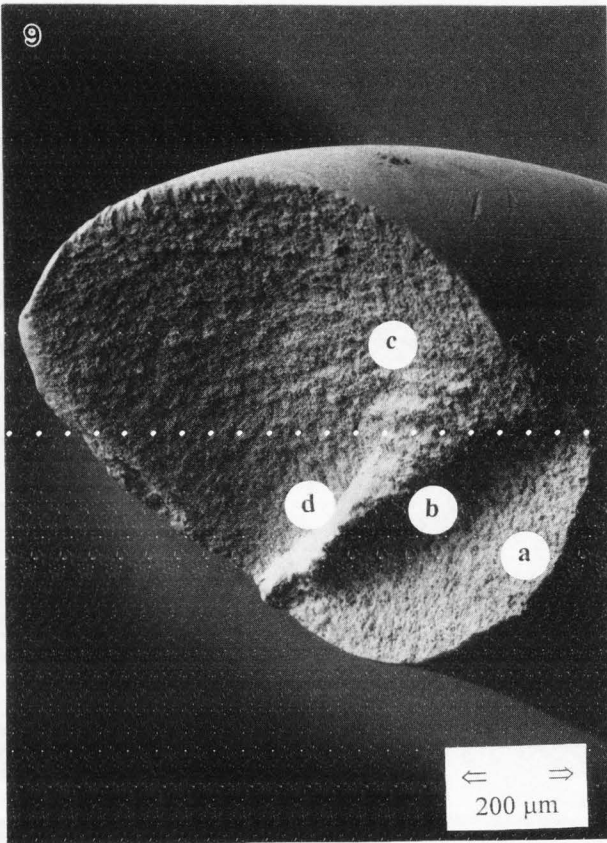
Figure 13. Scanning electron micrograph of polished and etched section of S204S hand scaler. Microstructure similar to Figures 5 and 6 for sonic scalers except for the absence of stringer inclusions.

----

over the entire fracture surface detected, at times, relatively high concentrations of Ca, Si, Al, and, at times, relatively strong concentrations of S, moderate concentrations of Mg and Cl, and relatively weak concentrations of Zn. The detection of Ca, Al, and Si qualitatively agreed with the spectra obtained from the as-polished section for inclusions shown in Figure 7.

Figures 9, 10, 11 and 12 present micrographs of the fracture surface from the clinically fractured S204S scaler. The surface topography contained a pronounced discontinuity. The surface is divided into four regions. Region a (Fig. 9) extends from the lower circular edge, where crack initiation occurred and corresponds to concave part of the instrument curvature, to where the surface became partially slanted upward. Region b, which is slanted upward, extends for only a short distance before region c commences. Figure 10 shows the granular appearance of region b compared to the dimpled appearance of region c. Fracture in region c initiated from the right side of the instrument and progressed in a circular fashion from the right side to the left side of the instrument (Fig. 9). Higher magnification of region c above

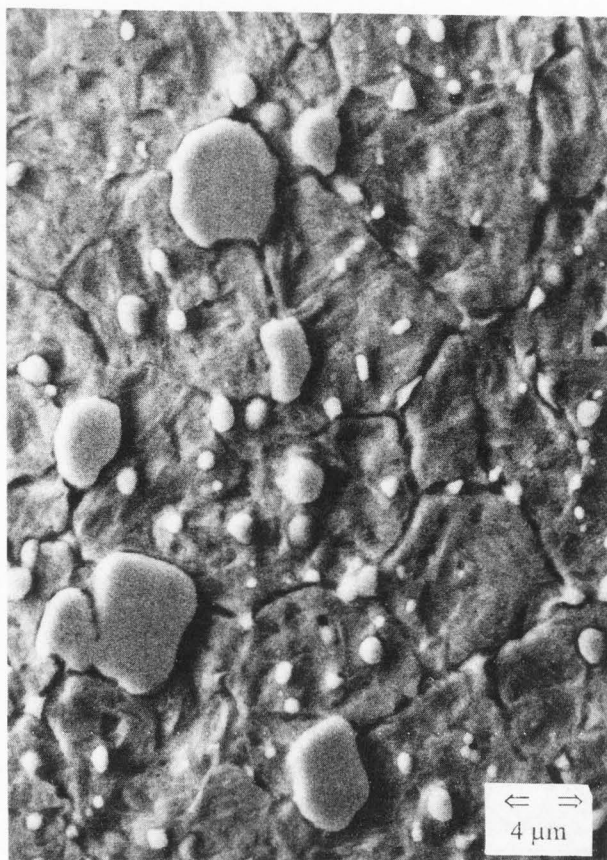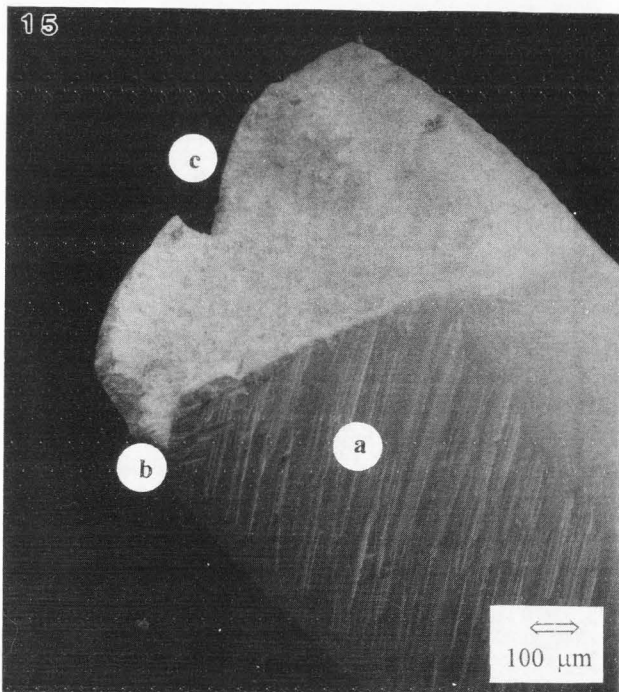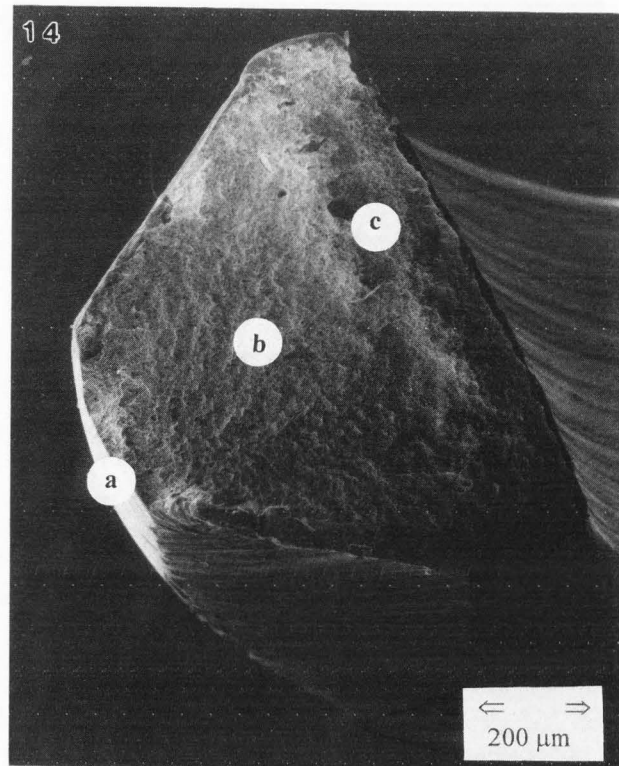Figures 14 and 15. Scanning electron micrographs of fracture surface from clinically retrieved SH6/7 hand scaler. Regions a, b, and c are identified in Figure 14. Figure 15 is taken at an optimum angle to reveal grinding grooves and their effects upon crack initiation and propagation: grinding grooves: a; crack initiation site: b; effects upon crack propagation: c.

Table 1. Vickers Microhardness (VHN)[1]

	as-rec[2]	ht[3]	center[4]	surf[5]	tip[6]	center[7]	fracture[8]	unused[9]
S204S	530 " 7	699 " 4	-	-	-	-	-	-
SH6/7	-	-	539 " 5	531 " 6	-	-	-	-
Sonic 1	-	-	-	-	585 " 6	570 " 4	560 " 9	-
Sonic 2	-	-	-	-	-	-	-	563 " 4
	a[10]	d	a	a	c	b	b	b

[1]Mean and standard deviation (n = 10).

[2]Near fracture plane of laboratory-broken tip in bending and corresponding to the opposite ended scaler tip from same instrument clinically broken.

[3]Broken tip in (1) above heat-treated in air at 1000°C for 1 hour and oil quenched.

[4]Near fracture plane but within interior of clinically retrieved instrument tip.

[5]Near fracture plane but near surface of instrument (3) above.

[6]Near tip of clinically retrieved instrument tip.

[7]Same as (5) but midway between tip and fracture plane.

[8]Same as (5) but near and along entire length of fracture plane.

[9]Indentations randomly taken along entire length of mounted scaler piece from tip to fracture plane.

[10]Columns with same letter are statistically similar and columns with different letters are statistically different at p ≤ 0.05.

---

the step is characterized by features shown in Figure 11. Here particles, both larger and smaller, are located at the bottoms of dimples. Finally, region d (Fig. 9), characterized by the flat surface of the step, is shown at higher magnification in Figure 12. The relatively flat step contained narrow and shallow grooves, observed as lines, running across its width. EDS analyses often yielded spectra across most of the fracture surface representative of particles and matrix, as detected on the etched surface shown in Figures 4, 5 and 6 for the sonic scaler.

Figure 13 presents the polished and etched microstructure for a section from the S204S broken scaler. Except for the absence of dark patches of longitudinal stringers, the microstructure is similar to the that of the sonic scalers shown in Figures 4, 5 and 6. Characterization of the polished and etched SH6/7 scaler revealed similarities to S204S. The larger particles from SH6/7, however, were only about one-half the size of those from S204S. Both of the non-sonic scalers revealed no stringer inclusions.

Figures 14 and 15 present low magnification micrographs of the fracture surface from the clinically retrieved SH6/7 scaler. Three regions characterize this surface. Region a represents the left part of the upper circular edge (Fig. 14) where crack initiation occurred.

Figure 15 shows that rough grinding grooves, occurring on the instrument sides, influenced the direction of fracture at initiation. Region b covers most of the fracture surface and includes the area where the crack radiated outwards and downwards from region a. Again, on the right instrument side, the occurrence of grinding grooves influenced crack propagation, as evidenced by the slanted edge over part of its length. Region c, corresponding to the bottom portion of the fracture surface just before the widest part of the instrument, is characterized by a slight elevation in surface and by a more granular appearance.

Table 1 presents the microhardness results. Both hand scalers, S204S and SH6/7 types, had similar hardnesses. For SH6/7, similar hardness occurred between interior and near-surface locations. For the clinically retrieved sonic scaler, slightly higher but statistically significant hardness compared to the S204S and SH6/7 hand scalers was found. The tip was found to be slightly harder (statistically significant) compared to the material near the center and fracture plane. For a new sonic scaler broken in bending in the laboratory, the mean hardness randomly measured along the entire length of the broken tip piece was similar to that of the clinically retrieved broken scaler. Finally, the broken S204S instrument tip, when heat treated at 1000°C in air for 1

hour and oil-quenched, displayed a relative increase in microhardness of 32%.

Discussion

The EDS analyses with a conventional X-ray detector (where elements with atomic number 11 and above can be detected) revealed very similar spectra for all three scaler types. The presence of Cr-rich Cr-Fe particles, the responsiveness of the scaler materials in microstructure and microhardness to thermal treatments, and the Fe-rich matrix composition containing 15.0-15.5% Cr by weight and without Ni, strongly suggest that the particles are carbides contained in a martensitic stainless steel (ASM, 1980). Even without detailed quantitative analyses for the bulk Cr contents, it is reasonable from the EDS analyses to assume that bulk Cr contents were several percent higher than the matrix contents, e.g., in the 16-18% Cr range. With this Cr content, the martensitic stainless steel is strongly suspected to be ASTM type 440 (ASM, 1980). The carbon content of this type is high and can occur in three ranges, starting at 0.60% and ending at 1.2%. Increased carbon content permits the formation of greater amounts of primary (islands) and secondary (particles) carbides during heat treatment. The amount, size, and distribution of carbides formed during heat treatment affect the properties obtainable from the hard as-quenched state. The carbide type known to form during quench and temper processing of martensitic stainless steels is $(Cr, Fe)_{23}C_6$, which begins to form at 480°C and is stable to high temperatures (Vander Voort and James, 1985). Another carbide of the $(Cr, Fe)_7C_3$ type also forms at 480°C but remains stable up to only 650°C. The latter carbide is to be avoided during thermal processing since it degrades properties, especially corrosion resistance. When thermal processing of hardened steels occurs at lower temperatures, $(Cr, Fe)C_3$ carbides form and are stable up to only about 480°C. The 440 type of martensitic stainless steels can also contain up to 1.0% Mn (max), 1.0% Si (max), 0.75% Mo (max), 0.04% P (max), and 0.030% S (max). Since the carbide particles contained about 1.0% S, this element was concentrated within the carbide phase. Mn, Si, Mo, and P were not detected. With the EDS technique used, detection limits of several tenths of a percent existed. Hence, although not detected, the steels may have contained low levels (below 0.2-0.4%) of these undetected elements.

Heat treating the S204S scaler at 1000°C for 1 hour followed by an oil quench essentially corresponded to transforming the steel to austenite followed by fully hardening the steel. The increased hardness (by 32%) showed the large range in mechanical properties potentially obtainable through metallurgical processing. By quenching the austenite structure from high temperature to room temperature, platelets of martensite formed, giving high hardness to the steel; these martensitic platelets can be observed within the grains of the etched structure in Figures 5 and 6. Reheating the hardened steel to temperatures up to about 480°C has the potential to relieve stresses built-up within the strained martensitic platelets, while reheating in the 540-650°C range tempers the structure by resizing and redistributing the carbide particles so that more desirable properties for useful applications can be obtained. Hence, it is essentially the latter operations that are variable under the control of the manufacturer and crucial in processing instruments with optimum dental performance. The martensitic stainless steels are sensitive to heat treating variables. Rejection rates due to faults in heat treating can be high (ASM, 1981).

According to ANSI/ADA Specification No. 64 on dental explorers, the martensitic stainless steel to be used for the working end shall consist of B, C, D, and other grades, and correspond to Vickers hardness number (VHN) of 415-465 (B), 490-560 (C), 530-610 (D), and a minimum of 415 (other). ISO 7153/1 list these grades to comprise cutting instruments. Many of the recommended uses for the particular grades overlap. For example, bone curettes and scissors can be composed mainly of any grade, while scalpels and knives comprise D and other grades. The VHN for the three types of scalers used in this project can be regarded to lie entirely within grade D or partially be included in grades C and D.

Stringer inclusions in steels are not unusual (Vander Voort and James, 1985). A stringer can be (i) a microstructural configuration of alloy constituents, or (ii) foreign non-metallic material aligned in the direction of working during processing. Stringers composed of sulfides are deliberately put into the free machining steels to serve a useful purpose, and stringers of less desirable δ-ferrite often occur in tempered martensite. A few undesirable stringer types classified in the second category can be composed of oxides or slags left over from the steel-making process. Due to hot and/or cold working the steels, stringers are arranged in the direction of working, along the longitudinal axis for wires and bars. The stringer inclusions occurring with sonic scalers (Figs. 5, 6 and 7) are somewhat unusual in that large primary carbide islands alternately separated regions of stringer material. The presence of microstructural constituents of foreign origin, composed of Ca, Si, and Al, is a reason for concern. Additional elements, including S, Mg, and Cl may likewise be involved, but their presence or increased concentration on the fracture surface may be the result of contamination after fracture occurred. If this inclusion occurred only sparingly

throughout the microstructure, its presence could be overlooked. But because of its widespread occurrence (Fig. 5) throughout all four scalers of this type, reason exists to strongly suspect that an inferior lot of steel was used in making these instruments. While the presence of these foreign inclusions has not been unequivocally linked to degradation in properties such as hardness, caution nevertheless was generated. The mean microhardness of the sonic scaler was found to be about 6% higher than that of two other instruments of different design. Microhardness, however, may be a poor indicator for detecting the effects of inclusions on properties, since random positioning likely placed the Vickers indenter directly over inclusions in only a few measurements out of a total of ten. Because of the ease in dissolving away this phase due to chemical etching, the inclusions may be relatively soft. Furthermore, because of the brittle nature (Kerlins and Phillips, 1987) of the fracture surface, concern must be given to a possible structure-property relationship due to inclusion content. Figure 2b reveals a number of longitudinal microcracks on the sides of the broken sonic scaler that are highly suspected to have propagated between surface imperfections of the stringer type. Subsequent observation of a polished section perpendicular to the fracture surface of the scaler generated additional speculation. It was noticed that microcracks were projected from the fracture surface into the bulk via stringer inclusions, which acted as both crack initiation sites and as sites of facile crack propagation. Therefore, it is highly likely that the presence of a large numbers of stringers within the microstructures of sonic scalers resulted in inferior steel quality, which was a leading cause of the failure experienced by practitioners. Even if stringer inclusions were not the basis of scaler failures, sound metallurgical practice requires elimination of such inclusions or, at least, a substantial reduction in their amount.

With only a micohardness requirement in ANSI/ADA Specification No. 64, steel instruments with inferior microstructures can go undetected. Whether or not a correlation existed between microstructure and mechanical properties, improved microstructures with a reduction in stringer inclusion content is in order. The presence of stringer inclusions is also likely to elute ions contained within the stringer. Hence, elution of Ca, Al, Si, and possible other ions is likely to occur by exposure to saliva and contact with the oral soft and hard tissues. As noted above, microhardness is likely a poor indicator to monitor inclusion content within these microstructures. It is recommended that a microstructural requirement for a selected number of instruments be included in the appropriate specifications for steel instruments. Light or electron microscopy can be used. Quantifying the inclusion content by a comparison to photographic

standards or by an imaging analysis procedure can be developed. To reveal contrast between inclusions and steel matrix, one or several etchants should be made available that are effective for all steel compositions included within the specifications. Hence, a requirement of this type would not be restrictive in any way for impeding the introduction of newer type materials and instrument designs.

The fractographic analyses served a useful purpose in providing information about the way the scalers fractured and their stress state at the time of fracture. All three clinically retrieved sonic scalers led to the same conclusion regarding instrument loading and fracture. Fracture initiated at the corner on the convex side of the instrument curvature, suggesting that the scaler tip was being pushed up against an object such as a tooth at the time of failure. The ultrasonic vibrations induced within the instrument tip while under load may also have accelerated the initiation and propagation of cracks from mechanical cycling fatigue. With this scenario, tensile opening stresses, equivalent to mode I loading in fracture mechanics terminology (Anderson, 1991), was applied to the convex corner of the instrument. The presence of stringer inclusions may have resulted in preferred initiation sites. Once initiated, the crack propagated a short distance, as shown by the flat area (region a in Fig. 2), and then radiated outwards and almost perpendicular to the instrument sides. However, as the crack propagated, it soon required an adjustment in its direction in order to accommodate the changing direction of the applied force, which may have been generated by an inward bending and pushing of the instrument, as revealed by the partially slanted surface in region b. Soon thereafter, the conditions for brittle fracture were met, and fracture entered into region c where fast crack propagation occurred until the crack advanced almost to the top edge. Stringers within the microstructure accelerated brittle fracture within region c, as suggested by the presence of surface cracks running perpendicular to the fracture surface (Fig. 2b). Higher magnification of these surface cracks revealed numerous microcracks connected by stringer inclusions. Hence, brittle fracture may have occurred under the conditions imposed on the instrument due to a reduction in yield strength of the steel because of the presence of stringer inclusions. The remaining portion of unfailed material was unable to support any load that was still applied and easily fractured in a ductile manner, resulting in region d, with a shear lip.

Fractographic analysis of the S204S clinically retrieved scaler revealed more complexity in its loading pattern. Since crack initiation occurred on the concave side of the instrument curvature, it was inferred that the scaler was being pulled in bending, as might occur by

hooking the tip around an object while being pulled. In this manner, tensile opening stresses were applied to the concave surface, initiating a crack that propagated a short distance inwards (region a in Fig. 9). Both tensile (mode I) and in-plane shear stresses (mode II) were required to characterize the stress state of the system, since both pulling and bending took place. Hence the fracture plane was required to become slanted (region b) in order to accommodate both types of stresses. Shortly thereafter, however, the scaler must also have been subjected to a twisting motion that included out-of-plane shear stresses (mode III). At this point, the fracture entered region c, where crack propagation continued radially from the right to left side. As the crack was completing its semicircular path to the left side, the position of the crack generated in region c did not exactly meet the crack that had propagated on that side in region b. Hence, the last part of the instrument to fracture was the remaining small portion characterized by a flat step (region d). The shear lip existing on the upper left edge of the circular geometry supports the mechanism for region c.

For the clinically broken SH6/7 scaler, fractographic analysis revealed that the instrument was stressed by being pushed inwards since crack initiation occurred on the convex surface. The stress state consisted mainly of a tensile opening mode. Since the fracture propagated almost perpendicularly through the instrument, very little, if any, in-plane shear stresses occurred. Further, as the SH6/7 was pushed inwards, an inward rotation, also favoring this stress state, may have occurred. Moreover, since crack propagation occurred almost vertically from the top to the bottom edge, very little, if any, out-of-plane or twisting occurred. This scaler was the only example where the coarse grooves from grinding, still easily detected on the sides of the instrument, partially influenced the fracture direction. Since crack initiation occurred at a site influenced by grinding grooves (Fig. 15), it may be that fracture of this scaler was affected due to the concentration of stress at the site of the grinding grooves.

Besides materials properties, another reason for instrument fracture is the design of the instrument itself. Poor design involves ineffective geometries and insufficient cross-sectional bulk to support applied loads. Instruments are needed that do not suddenly break into distinct pieces but rather remain intact in one piece by plastically yielding when subjected to an overload situation. This can be accomplished by increasing the cross-sectional bulk and using materials with lower yield strengths and higher plasticities. Only the tips need to be hardened through controlled processing in order to provide effectiveness as dental scalers and in other uses. None of these issues are currently being addressed,

clearly, future research needs to consider these items.

Conclusions

(1). The quality of the martensitic stainless steel, very likely of the 440 type, comprising three clinically retrieved broken sonic scalers and one unused sonic scaler, was degraded due to the presence of stringer inclusions.

(2). The stringer inclusions were up to 50 μm in length and contained Ca, Al, and Si, and possibly S, Mg, and Cl, within some of the regions. The stringers were abundantly distributed within the microstructures and aligned in a longitudinal direction with the instrument axes as a result of the manufacturing process.

(3). It is believed the stringers led to brittle fractures, which occupied much of the fracture surface on each of the three clinically broken sonic scalers. Also, the stringers provided initiation sites for microcracks to form, and adjacent stringers provided paths for facile crack propagation.

(4). Microhardness requirements alone, which are used in ANSI/ADA specifications for these instruments, are inadequate to prevent the use of inferior quality steel such as that containing stringer inclusions. Recommendation is made that a microscopy requirement or another test also sensitive for the detection of stringer inclusions be added to the appropriate specifications.

(5). Two clinically retrieved and several unused hand scalers of the S204S and SH6/7 type were composed of steel of a grade similar to that of the sonic scalers, but of a higher quality steel free of stringer inclusions.

(6). The fracture features on the clinically broken scalers proved to be indicative of the stress states applied to the instruments at the time of fracture. The sonic and SH6/7 hand scalers were pushed or bent inwards, while S204S scaler tip was pulled with a twisting motion.

(7). The presence of coarse grinding grooves on the instrument sides is discouraged since crack initiation and propagation can be affected.

Acknowledgement

References

Anderson TL (1991) Fracture Mechanics, Fundamentals and Applications. CRC Press, Boca Raton, FL. pp. 58-60.

ANSI/ADA (1976) Specification No. 29: Hand Instruments. American Standards Institute, New York.

ANSI/ADA (1986) Specification No. 64: Dental Explorers. American Standards Institute, New York.

ASM (1980) Wrought stainless steel. In: Metals Handbook (Ninth Edition), Volume 3, Properties and Selection: Stainless Steels, Tool Materials and Special-Purpose Materials. American Society for Metals, Metals Park, OH. pp. 3-40.

ASM (1981) Heat treating of stainless steel. In: Metals Handbook (Ninth Edition), Volume 4, Heat Treating. American Society for Metals, Metals Park, OH. pp. 623-646.

Carroll DP (1993) Take extreme care when retrieving broken tips. RDH (Registered Dental Hygienist) 13(3): 38.

Geaman JR, Moser JB (1987) Hardness and metallurgical characterization of dental hand-cutting instruments. Dent Mater 3: 252-255.

Gettleman L, Renz E (1981) Hardness profiles of steel dental hand instruments, and possible rehardening methods. Quintessence Int 12: 223-230.

Ioannidis H (1990) Foreign bodies of dental origin in the gastrointestinal tract. Hellen Stomatol Chron 34: 53-55.

ISO 7153/1 (1983). Instruments for surgery: Metallic materials; Part I: Stainless steel. International Organization for Standardization, Geneva, Switzerland.

ISO 683/13 (1986). Heat-treatable steels, alloy steels and free-cutting steels; Part 13: Wrought stainless steel. International Organization for Standardization, Geneva, Switzerland.

Kerlins V, Phillips A (1987) Modes of fracture. In: Metals Handbook (Ninth Edition), Volume 12, Fractography. ASM International, Metals Park, OH. pp. 12-71.

Littner MM, Dayan D (1982) Foreign bodies of dental origin in the alimentary and respiratory tracts. Quintessence Int 13: 1001.

Mueller HJ (1996) Effect of surface preparation on high temperature oxidation of Ni-Cr-Be and Co-Cr alloys. Microstructural Sci 23: 197-205.

Nandi P, Ong GB (1978) Foreign bodies in the oesophagus: Review of 2394 cases. Br J Surg 65: 5-9.

Szabo M, Szabo I, Buris L (1972) Foreign bodies of dental origin in the oesophagus. Oral Surg 34: 196-200.

Thomas HF, Carr-Locke D (1989) The endoscopic removal of a dental reamer from the colon. Dent Update 16: 214-215.

Vander Voort GF, James HM (1985) Wrought stainless steels. In: Metals Handbook (Ninth Edition), Volume 9, Metallography and Microstructures. American Society for Metals, Metals Park, OH. pp. 279-296.

Editor's Note: All of the reviewer's concerns were appropriately addressed by text changes, hence there is no **Discussion with Reviewers.**